5 *Seeing* Giant Micelles by Cryogenic-Temperature Transmission Electron Microscopy (Cryo-TEM)

Yeshayahu (Ishi) Talmon

CONTENTS

5.1 INTRODUCTION

To fully characterize liquid, semiliquid, gel, or solid systems requires direct, supramolecular-level information, that is, images, which show how molecules assemble to form aggregates of various sizes and shapes. Cryogenic-temperature transmission electron microscopy (cryo-TEM) is an excellent tool to obtain direct imaging of liquid or semiliquid specimens, thermally fixed into a vitreous or quasi-solid state. Sample preparation for cryo-TEM makes it possible to preserve the nanostructure of the system in its native state while making it compatible with the stringent requirement of the microscope. Because cryo-TEM provides high-resolution direct images of the nanostructures and microstructures in the system, it can elucidate the nature of the basic building blocks that make up the systems, covering a wide range of length scales, from a few nanometers to several microns. Quite often many different types of assemblies coexist in the examined systems. Cryo-TEM makes it possible to observe them all, even those that are difficult to tell apart and identify by other, so-called indirect methods, such as

scattering techniques. The interpretation of cryo-TEM images is usually quite straightforward and not model dependent, whereas data interpretation in "indirect methods" is model dependent and is complicated when the system contains more than one type of aggregate or a broad size distribution.

In the case of micellar systems, including "giant micelles," cryo-TEM is most useful to image the range of the nanostructures present in those systems, for example, threadlike micelles (TLMs, also referred to as wormlike micelles, WLMs) coexisting with spheroidal micelles (SMs), branched TLMs, and TLMs that form loops or lassolike micelles. In some cases, reliable direct images provide the only way to prove a suggested or a theoretically predicted model. That was demonstrated, for example, in the case of the theoretically predicted branched micelles,[1] and the shape of the end-caps of threadlike micelles.[2,3]

It should be emphasized here that while micrographs are most useful, cryo-TEM is not a strictly quantitative technique. It is the technique of choice to determine the structural building blocks of complex fluid systems, but the quantitative data should be usually provided by other techniques, such as small-angle x-ray scattering (SAXS) and small-angle neutron scattering (SANS) (see Chapter 6), or nuclear magnetic resonance (NMR). Another advantage of these scattering techniques is that they probe the bulk of the system, not just a small sample of it; they thus provide a real statistical average. However, in a very heterogeneous system, such an average may be difficult to interpret. In addition, these techniques are "model dependent," not "observer dependent." Based on that, the best experimental approach is to apply cryo-TEM to study the nature of the nano-building blocks of the system, use that information to construct a physical model to be applied to interpret data from the above mentioned "indirect techniques," and then check whether the two sets of results from, say, scattering and TEM agree, to rule out possible artifacts.

The reader will find next a description of the basics of cryo-TEM, especially as it is applied to the study of "giant micelles." That is followed by a review of the applications of the technique in the study of the systems in the focus of this book. The interested reader will find more details about the technique and its application to other systems in Talmon[4] and Danino.[5]

5.2 BASICS OF DIRECT-IMAGING CRYO-TEM

The term cryo-TEM covers the two main techniques that involve fast cooling of the specimen as part of its preparation before it is examined in the TEM. The more widely used technique is "direct-imaging cryo-TEM," which involves fast cooling of a thin specimen and its transfer at cryogenic temperature into the TEM, where it is maintained and observed at cryogenic temperature. Alternatively, a larger sample of the system is quickly cooled, the frozen sample is fractured, and a thin metal-carbon replica is prepared of the fracture surface. Then the sample is melted away, the replica is cleaned and dried and observed in the TEM at room temperature. That is called "freeze-fracture-replication cryo-TEM," or, in short, FFR.

This section describes in some detail the basics of direct-imaging cryo-TEM. FFR is described in the next section of the chapter. Some of the considerations involved in cryo-TEM do apply to both classes and are described in the current section.

Samples that contain high concentrations of liquids must be made compatible with the TEM. It is necessary to lower the vapor pressure of these systems to make them compatible with the high vacuum in the microscope column, typically better than 10^{-6} Pa. Also, any supramolecular motion must be stopped to prevent blurring of the recorded image. Of course, all TEM specimens must be thin, not thicker than about 300 nm, for the usual accelerating voltage of 120 kV. Thicker specimens give rise to inelastic electron scattering that deteriorates image quality. However, inelastically scattered electrons may be filtered out in those electron microscopes that are equipped with an in-column or post-column energy filter.

The reduction of vapor pressure and arresting supramolecular motion is called "fixation," that can be either chemical or physical (thermal). Chemical fixation involves addition of a chemical substance alien to the sample. Because nanostructured liquids, particularly surfactant-based systems, are very sensitive to changes in composition, addition of compounds such as a stain (a substance that enhances contrast) or fixative, followed in some cases by a chemical reaction between the fixative and the specimen, and often by drying of sample, may alter the original nanostructures in the system. Thus, chemical fixation is unacceptable (in most cases) for the study of nanostructured liquids. Hence, the method of choice is thermal fixation, that is, ultrafast cooling of the liquid specimens into a vitrified or quasi-solid state. This is achieved by rapidly plunging the specimen into a suitable cryogen. Because thermal diffusivities are larger than mass diffusivities, thermal fixation is much more rapid than chemical fixation, and, of course, eliminates the addition of an alien compound to the system.

The cooling rate needed for vitrification of water is on the order of 10^5 K/s, as estimated theoretically.[6] The cooling rate during vitrification was measured experimentally in an actual specimen preparation setup,[7] and was indeed found to be the order of 10^5 K/s. When cooling is too slow, crystalline ice, hexagonal or cubic, forms in aqueous systems. In nonaqueous systems, various other crystalline matrices may form in the cooled specimen. Crystalline matrix causes optical artifacts, mechanical damage to the microstructure, and redistribution of solutes. Solutes are often expelled from the growing ice lattice, and are deposited either in the crystal grains or, often, at grain boundaries.

The high cooling rates needed for vitrification require very large surface-area-to-volume ratio. To achieve that, the geometry of choice is a thin film. The limited penetration power of even high-energy electrons also requires thin films (up to 300 nm thick, as stated above). High-resolution imaging requires thinner samples. In practice most direct-imaging vitrified specimens display a wide thickness range. While microscopes operating at 200, 300, and 400 kV are capable of imaging specimens thicker than specified above, image interpretation becomes increasingly more difficult with specimen thickness. It is the high depth of field of the TEM that leads to superposition of information from many layers of thick

specimens, all projected onto the plane of the detector. In FFR, samples are usually much thicker, thus cooling rates are slower and vitrification is rarely achieved.

The cryogen needed to successfully vitrify the specimen has to be at a low temperature, and well below its boiling point to avoid formation of a gas film around the specimen during quenching; such a gas film acts as a thermal insulator (the Leidenfrost effect). A good cryogen also has high thermal conductivity. Liquid nitrogen is a poor cryogen for most applications (see exceptions below), because of the narrow temperature range between its freezing and boiling. In contrast, liquid ethane, cooled to its freezing point (−183°C) by liquid nitrogen, is an excellent cryogen (its normal boiling point is about 100 K higher).

Another important issue in cryo-TEM preparation is the preservation of the nanostructure at precise conditions, namely, temperature and concentration. This cannot be achieved unless the specimen is prepared in a controlled environment of the desired temperature and atmosphere that prevents loss of volatiles, for example, water vapor. This requires a so-called controlled-environment vitrification system (CEVS). Several models are available, especially the relatively simple, but very reliable system developed by Bellare et al.[8] and modified by Talmon and co-workers over the years,[7,9] and the automatic "Vitrobot" of the FEI company that was developed by Frederik and co-workers.[10] The former CEVS can be used from −10 to +70°C and with various saturated or unsaturated atmospheres. It can be used for the preparation of FFR specimens, too.

Cryo-TEM specimen preparation is performed inside the CEVS, where the atmosphere is closed and controlled from the outside. A small drop, typically 3 to 5 μL, of a pre-equilibrated system is pipetted onto a perforated carbon film, supported on a TEM copper grid, held by tweezers and mounted on a spring-loaded plunger. Most of the liquid is blotted away by a piece of filter paper wrapped around a metal strip, leaving thin liquid films supported on the hole edges of the perforated carbon film. After blotting, the plunging mechanism is activated, a trap door opens simultaneously, the specimen is driven into the cryogen and is vitrified. Finally, the vitrified sample is transferred under liquid nitrogen to the working station of a cooling holder, where it is loaded into the special holder and transferred into the microscope. In some cases, a bare grid (i.e., a microscope grid not covered by a perforated film) is used. More technical details can be found elsewhere.[4,8]

The blotting step is very important for successful sample preparation. It may be performed in a number of ways. The simplest is wicking most of the liquid by simply touching the filter paper to the edge of the grid carrying the drop. Viscoelastic fluids, for example, TLM solutions, require blotting with a shearing or smearing action. That temporarily reduces the viscosity of a shear-thinning liquid, allowing the formation of a thin enough liquid film on the support. Another option is to press two pieces of blotting paper on the two sides of the specimen; that can be performed either manually or, as in the case of the Vitrobot, automatically. That mode usually produces more uniform films. The blotting process and the confinement of the liquid in a thin specimen may introduce artifacts one

should be aware of (see below). In addition to changes of the nature of the nanostructure, distortions of large objects, and alignment of slender "one-dimensional" (rods or threads) or large "two-dimensional" (sheets) objects may take place.

After blotting, while the thin specimen is still liquid, it may be kept in the controlled environment of the CEVS for some time. In the case of many self-aggregating systems such as TLMs, this allows the specimen to relax after shear and elongation it may undergo during blotting.[11,12] The specimen may also undergo different processes directly on the grid, including chemical or physical reactions induced by different triggers such as fast heating[7,9] or cooling,[13] pH jumps,[14] or gelation. Those processes may be stopped at any intermediate stage by plunging the specimen into the cryogen. The experiment may be repeated a number of times, each time allowing the process to proceed further towards completion. That way one obtains a sequence of vitrified specimens that gives time sectioning of the process. This is called "time-resolved cryo-TEM." Several variations of the CEVS have been built to facilitate such experiments.[7,9,15] In the case of self-aggregating systems, when one is interested in high-viscosity phases that cannot be directly made into a thin liquid film, on-the-grid cooling (or, in rare cases, heating) is a convenient way to produce high-viscosity phases on the grid, starting with a low-viscosity precursor.

There is an increasing interest in self-aggregation, including giant micelle formation, in nonaqueous systems. While direct-imaging cryo-TEM can be extended to nonaqueous systems, liquid ethane, the cryogen of choice, cannot be used in many cases because it is a good solvent for many nonpolar liquids. However, a good number of systems, such as those of branched hydrocarbons, aromatics, or systems that contain glycerides, do not crystallize readily upon cooling, and thus can be vitrified even in liquid nitrogen.[16] That is also true for aqueous systems containing sufficiently high concentrations of glycols (> 20%).[17]

5.3 FREEZE-FRACTURE-REPLICATION

As described above, freeze-fracture-replication (FFR) is an indirect route to cryo-TEM. As in direct-imaging cryo-TEM, FFR involves fast cooling of the specimen in an appropriate cryogen. However, the specimen is larger than that of the former technique, thus in most cases vitrification is not accomplished, and freezing artifacts should to be taken into consideration. The next step of FFR involves fracturing the frozen specimen, followed by the preparation of a metal-carbon replica of the fracture surface by vapor deposition. Fracturing and replication are performed in a vacuum chamber, while the specimen is kept at cryogenic temperature, typically below −150°C. First, a heavy-metal (typically platinum or a mixture of platinum and carbon) is deposited, usually at an angle of 45° to the horizon. This enhances contrast by a "shadowing" effect. A smaller angle is needed to bring out finer details. Then a carbon layer is deposited perpendicularly to the specimen to enhance the mechanical stability of the replica. In modern equipment the sources for the deposition of the metal and carbon are electron

guns bombarding a suitable target. An additional preparation option before replication is "etching," namely, removal of high vapor-pressure components. This requires warming up the specimen for a few minutes to about –100°C in the case of aqueous systems, a temperature at which the vapor pressure of ice becomes sufficiently high to give an appreciable rate of sublimation. After replication, the sample is melted, the replica is cleaned, collected on a TEM copper grid, dried, and imaged in the TEM at room temperature. In most laboratories that perform FFR, the entire process of fracturing the specimen and replication is carried out in commercially available systems. Fast cooling may be carried out in the CEVS to allow quenching from given, well controlled, conditions.[18] FFR is most useful when relatively high-resolution images are needed, but direct-imaging cryo-TEM is not practicable, for example, in the case of high-viscosity systems, or systems containing large particles that cannot be accommodated in the thin specimens of direct-imaging cryo-TEM. Of course, fine details or fine particles can be imaged by the technique. In fact, one early success in imaging a network structure of molecular organogel was achieved by applying the FFR technique in the study of a steroid/cyclohexane physical gel by Wade et al.[19] While the technique is excellent to complement direct-imaging cryo-TEM,[20] it has lost popularity in the last two decades and, regrettably, is used in only a few research laboratories. The reasons are that the technique is labor intensive, it relies more than many other techniques on the technical skills of the user, and it requires complex and quite expensive equipment. In recent years the commercial FFR units on the market need modifications before they can be successfully used. The gradual disappearance of the techniques is quite unfortunate, because FFR-TEM is a most useful imaging technique.

5.4 LIMITATIONS, PRECAUTIONS, AND ARTIFACTS

While cryo-TEM, both in the direct imaging and the FFR modes, is probably the most reliable technique to obtain direct, nanometric-resolution images of liquid systems, it cannot always be applied, and, despite all the precautions, the user has to be aware of possible artifacts. The experienced user knows when the technique can be applied and is able to distinguish between real nanostructures and artifacts. Sometimes the distinction is not easy, and data from other techniques should be compared to the physical model emerging from the micrographs.

It has been already mentioned that high-viscosity systems cannot be made into thin direct-imaging cryo-TEM specimens, but can be made into FFR cryo-TEM replicas. It is worthwhile restating here that shear-thinning viscoelastic liquids can be made into thin liquid films, even if their zero-shear viscosity is high. Care must be taken to allow sufficient relaxation time on the grid, prior to vitrification, to avoid flow-induced structures. Knowing the relaxation time of the system is most useful in such cases.

Occasionally, one works close to a phase boundary. In that case chemical-potential control of the gas phase in the CEVS becomes very important. If possible, one should saturate the atmosphere in the CEVS with the same kind

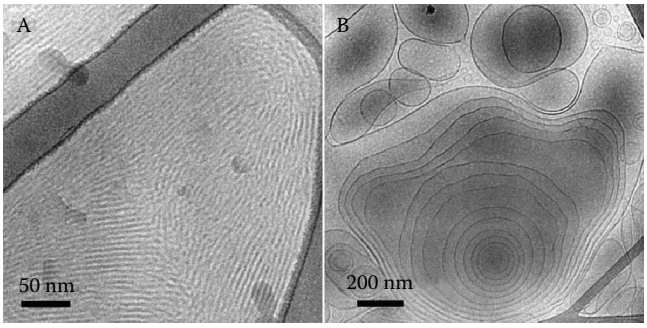

FIGURE 5.1 Vitrified specimens of 90 mM C_{14}DMAO, 10 mM SDS, and 200 mM heptanol in water. (A) Specimen prepared in an environment lacking the alcohol, after 90 seconds of relaxation following blotting, showing TLMs, aligned by the flow during blotting. (B) The same system prepared by the same protocol, but in a properly saturated atmosphere, showing multilamellar liposomes.

of solution as the one used to prepare specimens. In many cases, when only surfactants or polymers at low concentrations in water are used, the chamber may be saturated with pure water. However, if other volatiles are present in the mix, such as a low molecular weight cosurfactant, failing to use the actual studied solution for saturation may lead to artifacts. An example is shown in Figure 5.1 of the system made of 90 mM C_{14}DMAO (tetradecyl N,N-dimethylammonium N-oxide), 10 mM sodium dodecylsulfate (SDS), and 200 mM heptanol in water, whereas in Figure 5.1A we see a sample prepared in an environment lacking the alcohol, after 90 seconds of relaxation following blotting, and Figure 5.1B shows the same system prepared by the same protocol in a properly saturated atmosphere. The TLMs that are formed in this case are an artifact; the vesicles imaged in the properly executed experiment are the real nanostructures in this system. Note another artifact in this case: the alignment of the TLMs in Figure 5.1A, a result of flow during the blotting stage of the specimen preparation.

Contrast is an important factor in any TEM technique. In cryo-TEM this is especially crucial, as in most cases inherent contrast in the systems studied is low. The contrast becomes even lower when the continuous phase is not pure water, but a mixture of water and relatively high percentage of organic materials such as ethylene glycol or glycerol. At high concentration of glycerol (about 30 wt% and higher), TLMs become practically invisible, as contrast becomes close to zero. Contrast is also quite poor in organic solvents, although in many cases reasonable images can be recorded. In some organic solvents contrast is reversed, that is, the continuous phase is more optically dense than the nano-aggregate. An example is given in Figure 5.2 showing TLMs of 1% polystyrene-poly(isobutylene) diblock copolymer (molecular weight of 13000 : 79000) in a 1:1 mixture of dibutyl and diethyl phthalates.[21] Note the background of the vitrified phthalates

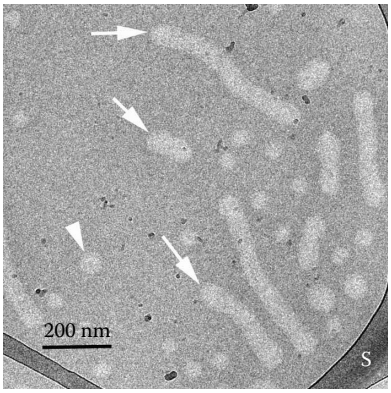

FIGURE 5.2 Cryo-TEM image of 1% polystyrene-poly(isobutylene) diblock copolymer (molecular weight of 13000 : 79000) in a 1:1 mixture of dibutyl and diethyl phthalates.[21] Note swollen end-caps of the TLMs (arrows), and the coexistence of TLMs with spheroidal micelles (arrowheads).

is more optically dense than the micelles. An interesting feature here are the swollen endcaps of the TLMs (arrows), and the coexistence of TLMs with spheroidal micelles (arrowheads). With increasing acceleration voltage in the TEM micrograph, contrast is reduced. For imaging soft materials we prefer to work at the moderately low acceleration voltage of 120 kV, whereas for high resolution TEM of "hard materials," higher acceleration voltage of up to 400 kV usually gives better results.

To overcome the poor contrast in vitrified cryo-TEM specimens, we almost always use "phase contrast," which is equivalent in principle to phase contrast in light microscopy, namely, enhancing contrast by converting phase differences to amplitude differences. In the electron microscope, phase contrast is formed by defocusing the microscope objective lens. This must be applied with care to avoid loss of resolution and introduction of imaging artifacts.

Normally, we refrain from enhancing contrast by staining, that is, adding a high-optical-density material to the system, in the hope that it will selectively attach to certain domains in the specimen; this is similar to biological specimens staining in light microscopy. Because most electron microscopy stains are either salts or acids of heavy elements, their addition to the system may alter its nanostructure. However, in some cases one can change the system slightly, with little effect on the nanostructure, in order to image the desired structures. In the case of ionic surfactants, one can often safely replace the light sodium ions with the much heavier cesium ions, or chloride ions with bromide ones. Of course, one should follow closely any possible structural changes caused by that substitution. An example where contrast was enhanced by replacing Na^+ by Cs^+ is given by Wittemann et al.[22] in the case of polymer brushes attached to polystyrene latex, a situation not unlike that of TLMs. Another example is shown in Figure 5.3 for

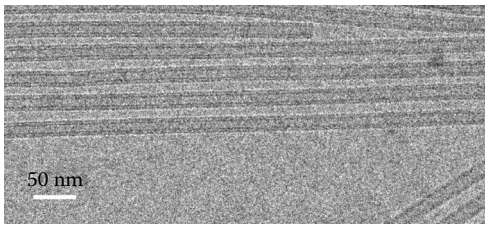

FIGURE 5.3 Nanotubes or tubular TLMs formed by complexation of 9 mM ionic block copolymer Eusolex with 1 mM cetyltrimethylammonium bromide (CTAB).[23]

tubular TLMs (essentially a nanotube) formed by complexation of the ionic block copolymer Eusolex (9 mM solution) with cetyltrimethylammonium bromide (CTAB 1mM). Note the fine structure, each wall exhibits two fine lines, visible thanks to the enhanced contrast of the Br^- ions. Those lines are most probably domains rich in the bromine anions.[23]

Another limitation for imaging, a possible source of artifacts, but occasionally a means to enhance contrast is electron-beam radiation damage. Organic compounds in vitrified aqueous or nonaqueous matrices are very susceptible to the electron beam.[24,25] Thus, all images must be recorded at low-dose conditions, namely at an exposure of just a few electrons per $Å^2$. Higher exposures to the electron beam may give rise to destruction of finer details, as demonstrated in Figure 5.4, to formation of new artifactual structures, or, as been shown in some solvents, to loss or reversal of contrast.[25] The threadlike micelles shown in Figure 5.4 were recorded by direct imaging cryo-TEM in an aqueous solution of 5 mM cetyltrimethylammonium chloride (CTAC) with 3 mM Na-p-iodobenzoate. In comparing the low-dose image (Figure 5.4A) with the high-dose image

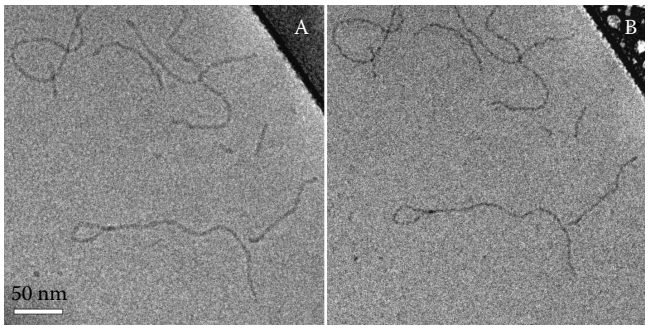

FIGURE 5.4 Threadlike micelles in a cryo-TEM image of an aqueous solution of 5 mM cetyltrimethylammonium chloride (CTAC) with 3 mM Na-p-iodobenzoate. Compare the low-dose image (A) with the high-dose image (B) and note the overall loss of material and fine detail. Note also the "lasso-type" TLM seen in this field of view.

(Figure 5.4B) note the overall loss of material and fine detail. Note also the "lasso-type" TLM seen in this field of view. Electron-beam radiation damage is certainly a problem in direct-imaging cryo-TEM. However, because radiolysis takes place preferentially at the organic material–vitrified water interface, careful exposure by the electron beam can "develop" contrast in areas where it is minimal.[26]

Finally, one should bear in mind that TEM is not strictly a quantitative technique (electron diffraction and lattice-imaging are exceptions). Image magnification depends rather strongly on the position of the imaged area on the optical axis of the microscope. Slight deviations from the ideal position (the "eucentric plan") give rise to changes in magnification that can be as high as ±10%; that is coupled by errors due to calibration and electromagnetic lens hysteresis. Thus measurement taken from electron micrographs should always be backed by data from more quantitative techniques, such as x-ray or neutron scattering. However, a reliable physical model to interpret the data for the latter techniques is to be based on the microscopy.

The apparent concentration one observes in cryo-TEM images may be misleading for two reasons. One is the redistribution of suspended aggregates in the liquid. Particles tend to move from thinner to thicker areas; in fact this is more so for larger particles, thus one observes also size segregation, with larger particles in larger number in the thicker areas while smaller one are left in the thinner areas. The second reason is the high depth-of-field mentioned above. It causes focused images of objects in different depths in the specimen to be simultaneously projected on the detector, thus giving the impression of higher concentration than the real one.

5.5 ADDITIONAL RECENT EXAMPLES

Several examples of the application of cryo-TEM in the study of giant micelles have been given above. The additional examples presented here are to illustrate the strength of the technique, and to serve as a guide to typical features often observed in images of "giant micelles." The reader may also find examples of the application of cryo-TEM in the study of various TLM systems in several chapters in this volume, for example, Chapters 7, 12, 14, and 16.

Figure 5.5 shows relatively high-magnification images of TLMs of the commercial cationic surfactant Habon G, which we studied some time ago.[5] White arrows in Figure 5.5A point to branching points, while white arrowheads point to overlap of two TLMs. The distinction between the two is made simple by paying close attention to the difference in appearance: while the branch has uniform optical density, the area of overlap is darker than the single TLM. Fresnel fringes (black arrowheads), an optical effect of interference between electrons traversing areas of high electron density (TLM) and lower density (vitrified ice), may also help distinguish between branches and points of overlap. The appearance of the Fresnel fringes, as well as the appearance of the entire images (contrast and resolution) depend on the amount of defocus of the TEM objective lens. Note that Figure 5.5B, showing the same system of Figure 5.5A, looks more grainy,

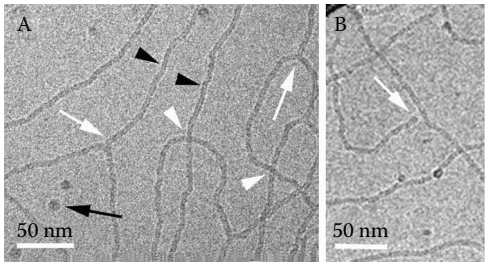

FIGURE 5.5 Cryo-TEM images of 0.1% commercial quaternary ammonium surfactant Habon G in water quenched from 20°C.[5] (A) White arrows point to branching points, while white arrowheads point to overlap of two TLMs. Fresnel fringes (black arrowheads) may also help distinguish between branches and points of overlap. Black arrow indicates a frost particle. (B) White arrow shapes a TLM end-cap, which is *not* hemispherical. Note that the image in A is more underfocused than the one in B.

and the Fresnel fringes look wider, the result of more defocus of the TEM objective lens. While the images in Figure 5.5 are quite clean, some small specks of frost (black arrow in Figure 5.5A) are visible. This is the result of water condensation on the cold specimen surface during specimen preparation and transfer. Good equipment and operator proficiency keep the amount of such contamination to a minimum.

Figure 5.5B shows a TLM tip (white arrow). In systems of very long TLMs such ends are difficult to locate in the image, especially in the case of relatively concentrated solutions where much overlap of the micelles occurs. Note the swollen so-called "end-cap" of the micelle, which does not form a hemisphere, as is quite often depicted in schematics of TLMs. Cryo-TEM has proven that the end caps are swollen, as shown here and in previous publications.[2,3] The same phenomenon can be seen in micelles in nonaqueous systems, as demonstrated in Figure 5.2 above.

The complementarity of direct-imaging cryo-TEM and freeze-fracture replication cryo-TEM (FFR) is demonstrated in Figure 5.6. It shows the evolution of the micellar structures observed in the mesoporous material SBA-15. The reaction mixture was sampled at different times after the addition of tetramethoxyorthosilane (TMOS) to an acidic (HCl) solution of Pluronic P123 held at 35°C.[20] Figure 5.6A is a direct-imaging cryo-TEM micrograph of the system after a short reaction time of 5'13''. The structure is that of spheroidal micelles. Due to the relatively high concentration, the projection of several layers of micelles on the TEM detector are observed and it is difficult to make out the individual micelles. After 14'05" the same technique shows TLMs (arrows in Figure 5.6B). In some areas of the micrograph we note the micelles were aligned by the flow during specimen preparation, while in other areas one sees the projection of randomly oriented TLMs. This is quite common in images of TLMs, especially at relatively high concentration. Freeze-fracture-replication of the system at about the same

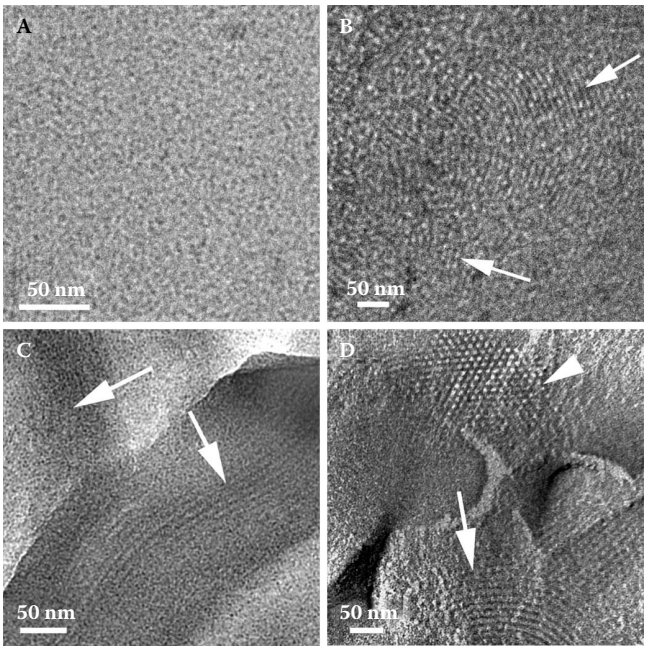

FIGURE 5.6 Evolution of nanostructure, as shown by cryo-TEM images of the SBA-15 reaction in HCl, vitrified from 35°C. (A) At t = 5'13" only spheroidal micelles are seen. (B) t = 14'05"; arrows show the TLMs. (C) Freeze-fracture-replication of the same system at t = 16'27"; arrows point to TLMs. (D) Same at t = 21'42". The hexagonal arrangement of the TLMs in this liquid crystalline phase is seen along their long axes (arrowhead), and the view perpendicular to the long axes (arrow).[20] Reproduced from Ref. 20 with permission of the American Chemical Society.

time of 16'27" (Figure 5.6C), also shows the TLMs (arrows). It is reassuring that the two techniques show the same nanostructures! At longer reaction times the system becomes too viscous because of liquid crystal formation, and it is impossible to image it by direct-imaging cryo-TEM; only FFR can be used. At 21'42" (Figure 5.6D) FFR reveals the arrangement of the TLMs into a hexagonal liquid crystalline phase. Note the hexagonal arrangement of the micelles seen along their long axes (arrowhead), and the view perpendicular to the long axis (arrow). While the spacings at 21'42" are very uniform, the nonuniform spacings between the TLMs in Figure 5.6C (16'27") indicate that those TLMs are, indeed, free.

In many surfactant-polymer systems threadlike micelles are formed. Quite often those TLMs arrange themselves into hexagonal liquid phases. Those complexes may be solubilized by excess surfactant to form free micelles. The evolution of phases, including TLMs in the system of poly(diallyldimethylammoniumchloride) (PDAC) and sodium dodecyl sulfate (SDS) was studies by

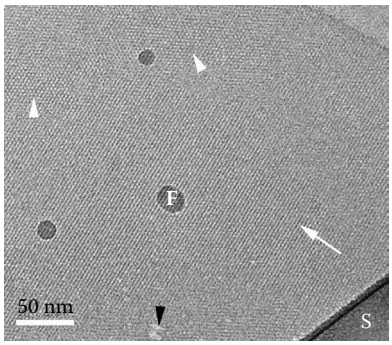

FIGURE 5.7 Vitrified specimen of the hexagonal liquid crystalline phase formed when CTAB is mixed at a charge ratio of 1:2 with 0.1 wt% PAAS. White arrow indicates the structure imaged perpendicularly to the long micelle axis; white arrowheads point to domains imaged parallel to the long axis. The black arrowhead indicates an area damaged by the beam. "F" is a frost particle. "S" is the edge of the support film.

Nizri et al.[27] In the reverse case of an anionic polyelectrolyte, poly(acrylic acid) sodium salt (PAAS), and various cationic surfactants, alkyltrimethylammonium bromides, the system has even a stronger propensity to form very long TLMs, ordered hexagonal arrays and nanoparticles of the hexagonal phase, depending on the surfactant hydrocarbon chain length and the polymer cation to surfactant anion ratio.[28] An example from this work is given in Figure 5.7, showing a very well developed array of the hexagonal phase made of the complexed TLMs. Some areas show hexagonal order (white arrowheads; the hexagonal phase imaged parallel to the TLMs long axes), while others are made of arrays of lines (white arrow; the phase imaged perpendicular to the TLMs). The order is not unlike what one observes by TEM of "hard-materials" crystals, but here we image a liquid crystalline phase in vitrified liquid state. The typical sizes here are nanometers, while in "hard" crystals the sizes are typically on the order of several Ångströms. These liquid crystalline phases are very electron-beam radiation-sensitive. Such images are recorded at very low electron exposures of not more than 15 $e^-/Å^2$, but some damage is already visible (black arrowhead).

Finally, in Figure 5.8 we see two direct cryo-TEM images of inverse TLMs of 0.38 wt% soybean lecithin in isooctane, vitrified in liquid nitrogen. The micelles are swollen by a small amount of water (0.02 wt%) that makes the packing of the lecithin in this form possible. These images, taken from an on-going project, show how the inverse micelles arrange themselves within the holes of the support film (Figure 5.8A). Their arrangement into a rather curious patterns, especially at the hole edge, as shown in Figure 5.8B, is, of course, an artifact of sample preparation. However that such images had not been seen before in other TLMs is especially intriguing, and is being further investigated.

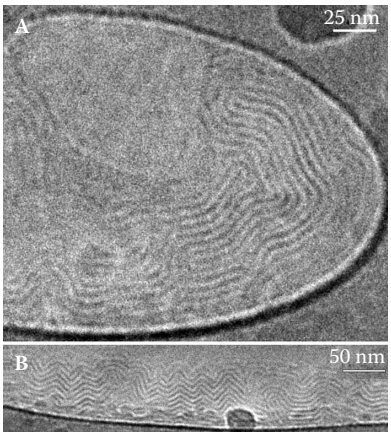

FIGURE 5.8 Two direct-imaging cryo-TEM images of inverse TLMs of 0.38 wt% soybean lecithin in isooctane, vitrified in liquid nitrogen. The micelles are swollen by a small amount of water (0.02 wt%).

5.6 CONCLUSIONS

Because of the complexity of giant micelle systems, namely, coexistence of TLM with spheroidal micelles, size distribution of TLM, branching and network formation, cryo-TEM is the best technique to capture directly all those features. The technique is mature now, with much of the basic physics behind it well understood, many of the technical difficulties solved, and a large number of possible artifacts well documented and avoided. Direct-imaging cryo-TEM is the most suitable cryo-technique for the study of giant micelles, but freeze-fracture-replication has been shown to be a useful complementary technique, especially for more viscous, gel-like systems. However cryo-microscopy requires expensive, sophisticated, and complicated equipment. Its applications require expertise, experience and technical dexterity, thus colloid science cryo-TEM is applied in just a few research centers. But the advent of nano- and bio-sciences that require the information the technique can afford, will no doubt make it much more available and accessible in the coming decade.

ACKNOWLEDGMENTS

My work on the cryo-TEM of threadlike micelles started back in 1985 in collaboration with Ted Davis and Skip Scriven of the University of Minnesota (my former Ph.D. advisors). I recorded the very first images of TLMs while on sabbatical in the laboratory of Wah Chiu, then at the University of Arizona, Tucson. Many other people have taken part in joint TLM related research projects ever since. Here I will just name a few who are represented in this chapter by images taken as part of those projects: Jack Zakin of the State University of Ohio,

Shlomo Magdassi of the Hebrew University of Jerusalem, Yachin Cohen of the Technion, Tim Lodge of the University of Minnesota, Heinz Hoffmann of the University of Bayreuth, Daniella Goldfarb of the Weizmann Institute, and Raoul Zana of the CNRS, Strasbourg, with whom we first identified branching in TLMs. Special thanks go to my former students, who are also represented here, and who are now faculty members, Dganit Danino of the Technion, Anne Bernheim-Groswasser of the Ben Gurion University, and to my current graduate student Alona Makarsky. The images of Figure 5.8 were taken by an undergraduate student working in my group, Mr. Ithai Lomholt-Levy. Last but not least I would like to express my gratitude to the permanent staff of my research group: Ellina Kesselman, Judith Schmidt, and Berta Shdemati.

REFERENCES

1. Danino, D., Talmon, Y., Levy, H., Beinert, G., Zana, R. *Science* 1995, *269*, 1420.
2. Bernheim-Groswasser, A., Zana, R., Talmon, Y. *J. Phys. Chem. B* 2000, *104*, 4005.
3. Zheng, Y., Won, Y.Y., Bates, F.S., Davis, H.T., Scriven, L.E., Talmon, Y. *J. Phys. Chem. B* 1999, *103*, 10331.
4. Talmon Y. In *Modern Characterization Methods of Surfactant Systems.* B.P. Binks, Ed., Marcel Dekker: New York, 1999, Chapter 5, p. 147.
5. Danino, D., Bernheim-Groswasser, A., Talmon, Y. *Colloid Surf. A* 2001, *183*, 113.
6. Uhlmann, D.R. *J. Non-Cryst. Solids* 1972, *7*, 337.
7. Siegel, D.P., Green, W.J., Talmon, Y. *Biophys. J.* 1994, *66*, 402.
8. Bellare, J.R., Davis, H.T., Scriven, L.E., Talmon, Y. *J. Electron Microsc. Techn.* 1988, *10*, 87.
9. Chestnut, M.H., Siegel, D.P., Burns, J.L., Talmon, Y. *Microsc. Res. Techn.* 1992, *20*, 95.
10. http://www.vitrobot.com/.
11. Danino, D., Talmon, Y., Zana, R. *Colloid Surf. A* 2000, *169*, 67.
12. Zheng, Y., Lin Z., Zakin, J.L., Talmon, Y., Davis, H.T. Scriven, L.E. *J. Phys. Chem. B* 2000, *104*, 5263.
13. Schmidt, J., Eger, S., Talmon Y. Manuscript in preparation.
14. Talmon, Y., Burns, J.L., Chestnut, M.H., Siegel, D.P. *J. Electron Microsc. Techn.* 1990, *14*, 6.
15. Fink, Y., Talmon, Y. In *Proc. 13th Int'l Congress on Electron Microsc.* 1994, 1: p. 37.
16. Danino, D., Gupta, R., Satyavolu, J., Talmon, *Y. J. Colloid Interface Sci.* 2002, *249*, 180.
17. Zhang, Y., Schmidt, J., Talmon, Y., Zakin, J. *J. Colloid Interface Sci.* 2005, *286*, 696.
18. Burns, J.L., Talmon, *Y. J. Electron Microsc. Techn.* 1988, *10*, 113.
19. Wade, R.H., P. Terech, P., Hewat, E.A., Ramasseul, R. Volino, *F. J. Colloid Interface Sci.* 1986*, 114*, 442.
20. Ruthstein, S., Schmidt, J., Kesselman, E., Talmon, Y., Goldfarb, D. *J. Am. Chem. Soc.* 2006, *128*, 3366.
21. Bang, J., Jain, S., Li, Z., Lodge. T.P, Pedersen, J.S., Kesselman, E., Talmon, Y. *Macromolecules* 2006, *39*, 1199.

22. Wittemann, A., Drechsler, M., Talmon, Y., Ballauff, M. *J. Am. Chem. Soc.,* 2005 *127*, 9688.
23. Hoffmann, H., Schmidt, J., Talmon, Y. Manuscript in preparation.
24. Talmon, Y., Adrian, M., Dubochet, J. *J. Microscopy* 1986, *141*, 375.
25. Kesselman, E., Talmon, Y., Bang, B., Abbas, S., Li, Z., Lodge, T.P. *Macromolecules* 2005, *38*, 6779.
26. Mortensen, K., Talmon, Y. *Macromolecules* 1995, *28*, 8829.
27. Nizri, G., Magdassi, S., Schmidt, J., Cohen, Y., Talmon, Y. *Langmuir* 2004, *20*, 4380.
28. Nizri, G., Magdassi, S., Schmidt, J., Talmon, Y. Manuscript in preparation.